INTERACTION OF POWERFUL ELECTRO-MAGNETIC FIELDS WITH BRAGG REFLECTORS*

I. Bahns[†], W. Hillert, P. Rauer, J. Rossbach, Universität Hamburg, Hamburg, Germany
H. Sinn, European XFEL GmbH, Schenefeld, Germany

Abstract

The interaction of an X-ray free electron laser (XFEL) with a Bragg Reflector can cause a change of the lattice constant, which has a direct influence on the stability of the reflection conditions [1] and can also excite modes of vibration [2]. The dynamical thermoelastic effects of the photon-matter-interaction are simulated with a finite-element-method (FEM) using the assumptions of continuums mechanics. To compare the simulation results with measured signals, a Michelson interferometer with ultra-fast photodiodes (risetime < 175 ps bandwith > 2 GHz) has been built up. To test the experimental setup in an in-house environment a pulsed UV laser is used to introduce a temporal displacement field in a silicon crystal created by about 0.26 µJ of absorbed energy. The measured signal is in agreement with the FEM simulation and has shown that if averaging over thousands of pulses is applied a resolution < 0.5 pm is feasible. This makes this experimental setup useful to investigate the X-ray-matter-interaction of Bragg reflectors at modern X-ray facilities.

INTRODUCTION

When electro-magnetic fields are interacting with an X-ray Bragg reflector, the absorbed part of the energy will cause a change of the local thermal energy of the crystal. Due to thermal expansion this also affects the value of the local lattice parameter, and due to Bragg's law this has a direct influence on the reflection conditions. To investigate such effects one method is to directly observe the temporal change of the lattice by using X-ray radiation [1]. However, for this experimental method a modern X-ray facility is needed where the beam time for experiments is mostly limited. An alternative method could be to use optical methods like thermoreflectance [3], the knife-edge method or interferometry [4]. In the present work a Michelson interferometer is tested in terms of the requirements for such a measurement. For the first test measurement, a pulsed UV laser introduced temporal change of the displacement on the backside of a silicon crystal was detected (Fig. 1). The temporal development of the displacement can be simulated with numerical methods like the finite-element-methode (FEM), which can solve the coupled partial differential equations of thermoelasticity using the assumption of continuum mechanics. These results can be compared with measured displacements such as presented in the present paper. This is useful to investigate the stability of an X-ray free electron laser oscillator [5].

EXPERIMENTAL SETUP

To built up a Michelson interferometer a linear polarized continuous wave laser operating at a wavelength of 532 nm is used. As illustrated in Fig. 1 polarizing beamsplitters (PBS) in combination with rotatable wave plates ($\lambda/2$ and $\lambda/4$) give control over the intensity, which is transmitted or reflected by the PBS. Film polarizers (FP) reduce the amount of intensity, which reaches the photo detector areas to the desired value. A PID controller stabilizes the working point of the interferometer by controlling the position of the mirror in the reference arm of the interferometer. Spherical lenses are used to collimate and focus the beam in a way that the focal plane lies on the surface of the silicon crystal and at the detector areas. Also the focal spot at the detector area is reduced to a size which is smaller than the area of the detector. The $\lambda/4$ wave plates are adjusted such that the total amount of the reflected beam of both interferometer arms goes into the direction of PBS3. The setup is adjusted in a way that the beam waists coming from each interferometer are equal. The beam size at the focal spot lying on the surface of the crystal and the reference mirror is ω_0=25 µm.
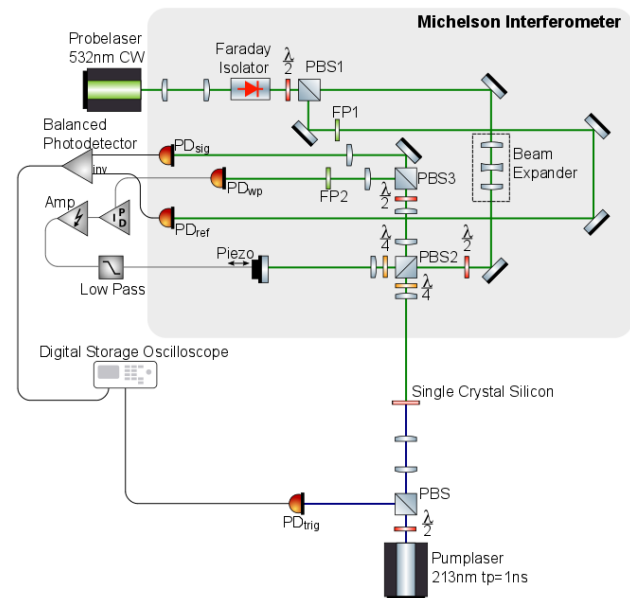

Figure 1: Pump-probe setup with Michelson interferometer. For a detailed description see the text.

The electric field amplitude and phase of the probe laser is described by using the Jones calculus:

$$\vec{J} = \begin{pmatrix} E_{0x}e^{i\varphi_x} \\ E_{0y}e^{i\varphi_y} \end{pmatrix} . \qquad (1)$$

Following Maxwell's equations the intensity in this case is proportional to $I \sim \mathbf{E}^{\dagger} \cdot \mathbf{E}$. With the $\lambda/2$ plate before the PBS2 the intensities coming from each interferometer arm are adjusted to be the same. Therefore the Jones vectors for the beams become:

$$\vec{J}_1 = \begin{pmatrix} E_0 e^{i\varphi_1} \\ 0 \end{pmatrix}, \qquad \vec{J}_2 = \begin{pmatrix} 0 \\ E_0 e^{i\varphi_2} \end{pmatrix}. \qquad (2)$$

Because the polarization states are perpendicular the beams won't interfere with each other. The intensity at this point is $I \sim 2E_0^2$. The fast axis of the $\lambda/2$ plate before PBS3 makes an angle of $\varphi = \pi/8$ with respect to the horizontal axis (x-direction), which gives considering the Jones Matrix [6], the following change of $\vec{J}_1$ and $\vec{J}_2$:

$$\vec{J}_1 = E_0 e^{i\varphi_1} \frac{1}{\sqrt{2}} \begin{pmatrix} -i \\ -i \end{pmatrix}, \quad \vec{J}_2 = E_0 e^{i\varphi_1} \frac{1}{\sqrt{2}} \begin{pmatrix} -i \\ i \end{pmatrix}. \quad (3)$$

The PBS3 transmits the vertical (y-direction) and reflects the horizontal (x-direction). So the transmitted intensity becomes $I_{tr} \sim E_0^2(1 - cos(\varphi_2 - \varphi_1))$ and the reflected $I_{ref} \sim E_0^2(1 + cos(\varphi_2 - \varphi_1))$. The phase difference $\phi = \varphi_2 - \varphi_1$ can be calibrated by changing the position Δz of one interferometer arm while holding the position of the other constant: $\phi = \frac{4\pi\Delta z}{\lambda}$. To achieve the optimal amplification performance of the balanced photo detector (BPD) both channels needs an input signal of $600\,\text{mV}$. This demands that the intensity of working point as well as the intensity reaching PD_{ref} must be adjusted with the help of the $\lambda/2$ plate before PBS1 and FD1 in a way that $600\,\text{mV}$ reaches each channel of the BPD. This calibration results in an output signal of $0\,\text{mV}$ if no pump signal is present. The reflected part of PBS3 is used to adjust the working point at the value between constructive and destructive interference. The considered displacements to be measured with this setup are below $1\,\text{nm}$, so the relation between voltage and displacement can be considered linear. The UV laser operates at a wavelength of $213\,\text{nm}$ and emits pules with a reparation of $1\,\text{kHz}$ and a pulse duration of $\approx 1.5\,\text{ns}$. With a thermal power meter an average power of $0.8\,\text{mW}$ has been measured, and the pulse energy therefore is $0.8\,\mu\text{J}$. Each pulse sents a trigger signal to a digital storage oscilloscope. The measured signal has been averaged over thousands of sweeps. The beam profile can be expressed with by a multi-Gaussian radial symmetric distribution and has been measured with an UV converter in combination with a beam profiler. The displacement signals created by the UV laser is measured with an ultrafast photodiode with a risetime $< 175\,\text{ps}$. In this work the first $60\,\text{ns}$ after the arrival of the UV laser pulse are measured. The results can be seen in Fig. 2 (a) The subplot shows the first $10\,\text{ns}$ before the trigger signal, where the displacement should be zero, indicating that the accuracy of the interferometer is below $0.5\,\text{pm}$. The silicon crystal has a area of $4\,\text{mm}$ x $10\,\text{mm}$ and a thickness of $100\,\mu\text{m}$

NUMERICAL SIMULATION OF DISPLACEMENT

The coupled non-linear[1] partial differential equations of thermoelasticity considering the infinitesimal strain theory under assumption of continuum mechanics and the Fourier heat law are used to simulate the displacement field of the above described measurement. Thermal losses by convection and radiation of the material surface are neglected. The simulations where carried out with the FEM software COMSOL Multiphysics® using the coupled *solid mechanics* and *heat transfer in solids* module. The absorption coefficient at $213\,\text{nm}$ has a value of $1.7884 \times 10^6\,\text{cm}^{-1}$ for silicon [7]. Due to the high value of the absorption coefficient the temporal and spatial function of the UV laser pulse is considered as a boundary heat flux:

$$Q(r,t) = \frac{E_{abs}}{2\pi(A\sigma_1^2 + B\sigma_2^2)}\left[Ae^{-\frac{r^2}{2\sigma_1^2}} + Be^{-\frac{r^2}{2\sigma_2^2}}\right]f(t). \quad (4)$$

The choice of multi-Gaussian function was necessary considering the measurement of the beam profiler. The data has been fitted to Eq. (4) using the software Origin® giving the values A=0.00544, B=0.01059, σ_1=57.634 µm, σ_2=18.748 µm. The function $f(t)$ in Eq. (4) is the temporal profile of the laser pulse. The integral of this function is normed to unity and contains discrete values, which have been measured with a fast photo diode. The interpolation between the values is piecewise cubic. Due to the refractive index 1.1222 and extinction coefficient 3.0314 [7] of silicon the reflectance is 0.67218 and therefore only E_{abs}=0.26 µJ are absorbed in the crystal. The temperature dependent values of thermal conductivity [8], thermal expansion coefficient [9] and the heat capacity [10] of silicon were taken from the cited publications. The following material parameters are considered temperature independent and taken fron the COMSOL material library: Poission's ratio ν=0.28 Young's modulus Y=170 GPa, ρ=density 2329 kg/m³. A radial symmetric simulation is considered with a mesh covering z=100 µm and r=700 µm. The mesh has quad elements of size=2 µm and a distributed boundary layer mesh at side where the heat source is applied.

The results of the simulation have shows that the strain σ_{zz} is about 10^{-5} and the strain σ_{rr} in the range of 10^{-6}. This shows that even small energy amounts (0.26 µJ) could have a significant effects considering the stability criteria for Bragg reflection because even strain of 10^{-7} can have noticeable effects on a Bragg reflection [1]. The dips in Fig. 2 (a), which occur in the measurement as well as in the simulations around 33 ns and 56 ns, give a time distance of 23 ns, which matches the time 23.5 ns observed by dividing twice the crystal thickness 100 µm by the longitudinal speed of sound $v_s = \sqrt{Y/\rho}$. The cause for this periodical dips are longitudinal ultrasonic waves, which are created by the dynamical thermal expansion due to the absorption of short laser pulse radiation. The ultrasonics are propagating with

---

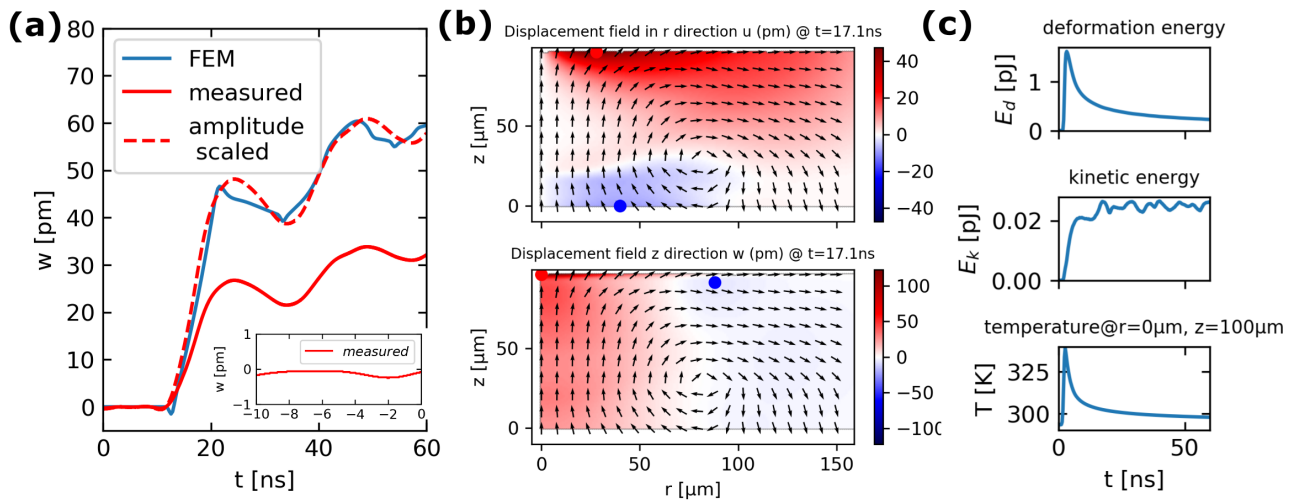1 Temperature dependence of material parameters is considered

Figure 2: (a) Comparison of the measured signal with FEM simulations. The broken line is the measured amplitude scaled to fit the simulation results. (b) Simulated displacement field inside the silicon crystal 17.1 ns after the photon matter interaction. The UV laser pulse arrives at z=100 μm with center (maximum intensity) at r=0 μm. The arrows are normed to a fixed value indicating the direction of the total displacement. The color code is set symmetric with white being the zero value. Maximum and minimum values are marked u_{max}=47.43 pm (red dot), u_{min}=−9 pm (blue dot), w_{max}=122.2 pm (red dot), w_{min}=−5.4 pm (blue dot). (c) Temporal evolution of the deformation energy, kinetic energy and the temperature value at r=0 pm, z=100 pm.

the speed of sound and are reflected at the boundaries of the crystal [11]. The simulated displacement at the backside illustrated in Fig. 2 (a) shows a similar form as the measured. However, the amplitude of the measurement is significantly smaller compared with the simulations. The reason could be that the used UV laser, after operating for some time, shows an intensity jitter, which lowers the mean energy per pulse. The general rise of the over all displacement, which is observed in the measurements as well as in the simulation can be explained by considering Fig. 2 (b). It shows the displacement field in the r and z direction at a time step 17 ns after the UV laser arrival at the top surface (at z=100 μm). The absorbed laser energy causes a rise in the temperature at the top of the crystal. Due to the spatial profile (Eq. (4)) of the laser the maximum temperature will occur at r=0 μm (Fig. 2 (c)). Due to thermal expansion, this causes a displacement field illustrated in Fig 2 (b). Because of the boundary conditions at the top (z=100 μm), the displacement w (in z-direction) will move upwards (positive z direction) and the displacement u (r direction) will move away from the center. However at the bottom (z=0 μm) the temperature is nearly the one of the initial value. This causes the backside of the crystal at r=0 μm, z=0 μm to move upwards. This is the area where the interferometer measures the displacement.

Considering the deformation energy and the kinetic energy[2] in Fig. 2 (c) it is seen that most of the deformation energy is caused by the thermal strain. The kinetic energy is about 0.025 pJ. The repetition rate of the laser is 1 kHz. Considering the crystal as a cantilever the first mode would be f=1.38 kHz. To have a rough estimation, which mean displacement u_m amplitude the crystal might have, the formula

---
[2] For definition of the deformation energy and kinetic energy see [2]

for kinetic energy is considered: $0.5M(2\pi f)^2 u_m^2$. With the mass of the crystal M=9.3 mg, u_m is some tens of nanometre. However, in this estimation passive damping is not considered. An observation of the measurement is, that at the start the displacement is nearly zero, which shows at least that the signal is not affected by vibrations. However, the measured signal is averaged and therefore further investigations considering mechanical vibration have to be carried out.

DISCUSSION AND OUTLOOK

Some of the assumptions made for the simulation like the Fourier heat law might not be not fully valid for the investigated system, e.g diffusion of the excess electrons and holes have to be considered. However, except for the modest amplitude scaling factor, the quantitative and the very good qualitative agreement between measurements and simulations indicate that the present results are a good starting point for more detailed investigations of Bragg reflectors with interferometer techniques.

REFERENCES

[1] S. Stoupin, A. M. March, H. Wen, D. A. Walko, Y. Li, E. M. Dufresne, S. A. Stepanov, et al., "Direct observation of dynamics of thermal expansion using pump-probe high-energy-resolution x-ray diffraction," Phys. Rev. B, vol. 86, no. 5, p. 054301, 2012. doi:10.1103/PhysRevB.86.054301

[2] B. Yang, S. Wang, and J. Wu, "Transient thermal stress wave and vibrational analyses of a thin diamond crystal for X-ray free-electron lasers under high-repetition-rate operation," J. Synchrotron Radiat., vol. 25, no. 1, pp. 166-176, 2018. doi:10.1107/S1600577517015466

39th Free Electron Laser Conf.　　　　FEL2019, Hamburg, Germany　　　　JACoW Publishing

ISBN: 978-3-95450-210-3　　　　　　　　　　　　　　　　doi:10.18429/JACoW-FEL2019-THP041

[3] Puqing Jiang, Xin Qian, and Ronggui Yang, "Tutorial: Time-domain thermoreflectance (TDTR) for thermal property characterization of bulk and thin film materials," *J. Appl. Phys.*, vol. 124, no. 16, p. 161103, 2018. `doi:10.1063/1.5046944`

[4] J-P. Monchalin, "Optical Detection of Ultrasound," *IEEE Trans. Ultrasonics Ferroelectrics and Frequency Control*, vol. 33, pp. 485-499, 1986. `doi:10.1109/T-UFFC.1986.26860`

[5] P. Rauer, I. Bahns, W. Hillert, J. Rossbach, W. Decking, and H. Sinn, "Integration of an XFELO at the European XFEL Facility," presented at the 39th Int. Free Electron Laser Conf. (FEL'19), Hamburg, Germany, Aug. 2019, paper TUP009, this conference.

[6] E. Hecht, in *Hecht optics*, Addison Wesley, 1998, pp. 213-214.

[7] D. E. Aspnes and A. A. Studna, "Dielectric functions and optical parameters of Si, Ge, GaP, GaAs, GaSb, InP, InAs, and InSb from 1.5 to 6.0 eV," *Phys. Rev. B*, vol. 27, no. 2, p. 985, 1983. `doi:10.1103/PhysRevB.27.985`

[8] C. J. Glassbrenner and Glen A. Slack, "Thermal Conductivity of Silicon and Germanium from 3°K to the Melting Point," *Phys. Rev.*, vol. 134, p. A1058, 1964. `doi:10.1103/PhysRev.134.A1058`

[9] Y. Okada and Y. Tokumaru, "Precise determination of lattice parameter and thermal expansion coefficient of silicon between 300 and 1500 K," *J. Appl. Phys.*, vol. 56, no. 2, pp. 314-320, 1984. `doi:10.1063/1.333965`

[10] H. R. Shanks, P. D. Maycock, P. H. Sidles, and G. C. Danielson, "Thermal Conductivity of Silicon from 300 to 1400°K," *Phys. Rev.*, vol. 130, p. 1743, 1963. `doi:/10.1103/PhysRev.130.1743`

[11] C. Thomsen, H. T. Grahn, J. M. Humphrey, and J. Tauc, "Surface generation and detection of phonons by picosecond light pulses," *Phys. Rev. B*, vol. 34, p. 4129, 1986. `doi:10.1103/PhysRevB.34.4129`